Nationaal Lucht- en Ruimtevaartlaboratorium
National Aerospace Laboratory NLR

Executive summary

Quantification of airframe noise using microphone arrays in open and closed wind tunnels

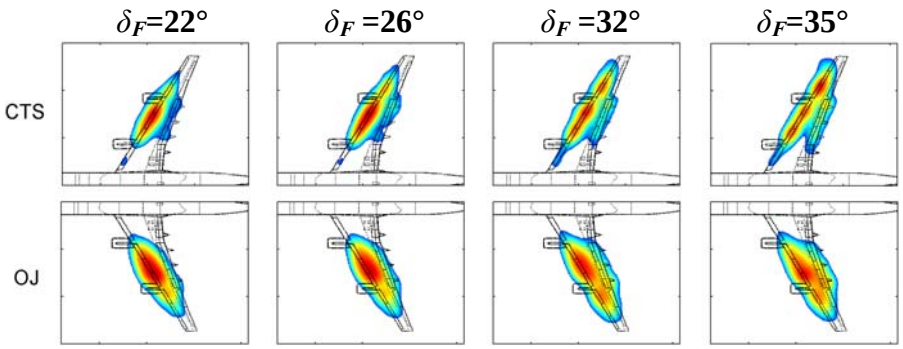

Problem area
While source location using phased microphone arrays has become a standard technique in aeroacoustics, the quantification of array results is still far from straightforward.

Description of work
The reliability of the phased array technique for quantifying airframe noise was assessed in the DNW-LLF open and closed wind tunnel sections. Acoustic measurements were performed on wing noise from a 1:10.6 scaled Airbus A340 model, using a 4-m diameter out-of-flow microphone array in the open jet and a 1-m diameter wall array in the closed test section.

Results and conclusions
Apart from the differences in array resolution, the source characteristics are generally similar for both test sections. The open jet results show that, although the absolute integrated array level can be too low due to e.g. coherence loss, the relative sound levels determined with the array (i.e. differences between configurations) are accurate within 0.5 dB. The difference between the absolute array levels in the closed test section and the farfield levels in the open jet is smaller than 3 dB for all frequencies. The relative array levels in the closed test section agree with the open jet within 1 dB, provided that the flow conditions - and therefore the noise source characteristics - are similar.

Applicability
This study has shown that reliable acoustic measurements in closed wind tunnel sections are possible.

Report no.
NLR-TP-2007-799

Author(s)
S. Oerlemans
L. Broersma
P. Sijtsma

Report classification
UNCLASSIFIED

Date
December 2007

Knowledge area(s)
Aeroacoustic & Experimental Aerodynamics

Descriptor(s)
MICROPHONE ARRAYS
WIND TUNNELS
AIRFRAME NOISE

This report is based on an article published in the International Journal of Aeroacoustics (2007), by Multi-Science.

Quantification of airframe noise using microphone arrays in open and closed wind tunnels

Nationaal Lucht- en Ruimtevaartlaboratorium, National Aerospace Laboratory NLR

Anthony Fokkerweg 2, 1059 CM Amsterdam,
P.O. Box 90502, 1006 BM Amsterdam, The Netherlands
Telephone +31 20 511 31 13, Fax +31 20 511 32 10, Web site: www.nlr.nl

Nationaal Lucht- en Ruimtevaartlaboratorium
National Aerospace Laboratory NLR

NLR-TP-2007-799

Quantification of airframe noise using microphone arrays in open and closed wind tunnels

S. Oerlemans, L. Broersma and P. Sijtsma

This report is based on an article published in the International Journal of Aeroacoustics (2007), by Multi-Science.

This publication has been refereed by the Advisory Committee AEROSPACE VEHICLES.

Customer	National Aerospace Laboratory NLR
Contract number	----
Owner	National Aerospace Laboratory NLR
Division	Aerospace Vehicles
Distribution	Unlimited
Classification of title	Unclassified
	March 2008

Approved by:

Author	Reviewer	Managing department
28/3/08	28-3-08	

Contents

ABSTRACT 5

NOMENCLATURE 5

1. INTRODUCTION 6

2. TEST SET-UP 7

3. DATA ACQUISITION AND PROCESSING 8

4. ABSOLUTE SOUND LEVELS 10
4.1 Source maps 10
4.2 Integrated spectra 10
4.3 Difference between array spectra and farfield levels 11

5. RELATIVE SOUND LEVELS 13

6. CONCLUSIONS 14

ACKNOWLEDGMENTS 14

FIGURES 15

REFERENCES 26

This page is intentionally left blank.

Quantification of airframe noise using microphone arrays in open and closed wind tunnels

Stefan Oerlemans, Liekele Broersma, Pieter Sijtsma
National Aerospace Laboratory NLR, Emmeloord, The Netherlands

ABSTRACT

The reliability of the phased array technique for quantifying airframe noise was assessed in the DNW-LLF open and closed wind tunnel sections. Acoustic measurements were performed on wing noise from a 1:10.6 scaled Airbus A340 model, using a 4-m diameter out-of-flow microphone array in the open jet and a 1-m diameter wall array in the closed test section. Apart from the differences in array resolution, the source characteristics are generally similar for both test sections. The open jet results show that, although the absolute integrated array level can be too low due to e.g. coherence loss, the relative sound levels determined with the array (i.e. differences between configurations) are accurate within 0.5 dB. The difference between the absolute array levels in the closed test section and the farfield levels in the open jet is smaller than 3 dB for all frequencies. The relative array levels in the closed test section agree with the open jet within 1 dB, provided that the flow conditions - and therefore the noise source characteristics - are similar.

NOMENCLATURE

A	Reconstructed source auto-power
AAAP	Average Array Auto-Powers (open jet)
B	Array size parameter: $r=B/f$ (with f in kHz)
C	Cross-Spectral Matrix
CTS	Closed Test Section
DNW-LLF	German-Dutch Wind Tunnels - Large Low-speed Facility
DR	Diagonal Removal
f	Frequency
$\mathbf{g}$	Steering vector
h	Scan grid index
H	Number of scan locations
L	Length scale for St normalization
m	Microphone index
n	Microphone index
N	Number of microphones
OJ	Open Jet
p	Complex pressure amplitude
P_{exp}	Integrated source power
P_{sim}	Simulated source power
PI	Power Integration
QCMB	Quarter-Circle Microphone Boom
r	Array radius
SNR	Signal-To-Noise ratio
SPL	Sound Pressure Level
St	Strouhal number
U	Wind speed
x	Speed exponent for wing noise
α	Aircraft angle of attack
δ_F	Flap angle
θ	Array opening angle

1. INTRODUCTION

Phased microphone arrays have become an important tool in aeroacoustic testing for their ability to localize and quantify different noise sources. Arrays are used in wind tunnels and in the field, and can be applied to stationary and moving objects. However, while source location has become a standard technique, the *quantification* of array results is still far from straightforward. For incoherent, separate monopole sources the absolute sound level corresponds to the peak level in the acoustic source map. However, in practice this situation seldom occurs. First, aeroacoustic noise sources are often spatially extended (e.g. slat noise, trailing edge noise). As a consequence, the peak levels in the source map depend on the extent and coherence of the source region and on the (frequency-dependent) resolution of the array. Second, the levels may be influenced by coherence loss between the microphones. Coherence loss can occur when sound is scattered by turbulence (e.g. in the shear layer of an open jet wind tunnel), and typically results in broader lobes with a reduced level in the source map. The effects of coherence loss increase with frequency, wind speed, and the distance between the array microphones. Apart from scattering by turbulence, coherence loss may also occur when the noise source does not radiate coherently in all directions. This effect increases with the opening angle of the array. Finally, the levels in the acoustic source map may be influenced by side lobes from other sources.

To overcome these complications, Mosher employed Dougherty's method for the quantification of array results[1]. She defined an integration area around the source region and calculated a frequency-dependent array calibration function, assuming a source distribution of uncorrelated monopoles. Brooks and Humphreys[2] extended this method, and applied it to simulations of a line source and to measurements of a calibrator source and flap side-edge noise. It was found that absolute spectra of different sources could well be recovered from the phased array results, and that coherence loss did not reduce the quality of the results significantly. However, the results were less reliable when the integration method was applied in combination with diagonal removal (DR). Diagonal removal[1] involves the removal of the main diagonal (i.e. the auto-powers) from the cross-spectral matrix, and is often inevitable in situations with low signal-to-noise ratio (e.g. a closed wind tunnel). An alternative method for reducing extraneous noise sources may involve the eigenvalue decomposition of the cross-spectral matrix, and removing the eigenvector(s) corresponding to unwanted noise[3].

An integration method similar to that of Brooks and Humphreys[2] was used by Soderman *et al*.[4] to determine the relative importance of different airframe noise sources in a closed wind tunnel. However, the reliability of the absolute and relative sound levels was not investigated, probably because single-microphone levels of the wall-mounted array were contaminated by flow noise. Blacodon and Elias[5] applied a quantification method to airframe noise in an open jet wind tunnel, and found good agreement of overall integrated levels with single-microphone spectra. However, their results may have been limited to low frequencies, where coherence loss effects are small. Furthermore, no source maps were shown for higher frequencies, where a high noise floor may have artificially increased the quantified array levels since no DR was applied[11].

Sijtsma and Stoker[6] extended the integration method to moving sound sources, and found that absolute levels can be accurately determined when auto-correlations (the time-domain equivalent of auto-powers) are included in the beamforming process. When auto-correlations were discarded, the integrated levels were too low, presumably due to suppression of secondary sources. Alternative array quantification methods, for linear noise sources such as trailing edge noise and slat noise, were presented in Refs. 7-10. Acoustic source maps were translated to absolute source levels using an array calibration function determined from simulations of an uncorrelated line source. In Ref. 10 good agreement between integrated array levels and single-microphone values was found for the frequency range where trailing edge noise was dominant (up to about 4 kHz). A drawback of these methods is that they are only suitable for line sources.

Oerlemans and Sijtsma[11] performed acoustic array measurements on wing noise from a 1:10.6 scaled Airbus A340 model in the open and closed test sections of the DNW-LLF wind tunnel. They used a modified version of the integration method from Ref. 2, which in case of DR discards negative 'source powers' in both the simulated and measured source plots. It was shown that in both test sections DR should be applied to obtain meaningful local source spectra, because without DR the results were obscured by uncorrelated noise in the main diagonal of the cross-spectral matrix. For the open jet the absolute integrated levels were found to be too low due to coherence loss, but relative levels (differences between configurations) could be determined accurately. Although the effective array size was reduced with increasing frequency to reduce coherence loss effects, the dependence of integrated levels on array size was not systematically investigated. In the closed test section coherence loss effects seemed to be small, but the reliability of absolute and relative levels could not be assessed because of flow noise on the wall-mounted array microphones. The array results for both test sections were not compared to each other because of changes to the model and wing devices.

It is worth noting that in the last years new deconvolution methods have been developed to increase the spatial resolution of phased microphone arrays[10-15]. Although these methods in principle account for resolution and side lobe effects, the calculated levels will still be affected by coherence loss. So even if fast and reliable algorithms are found, it is important to understand the different parameters influencing the reconstructed source levels.

The objective of the present study is to assess the reliability of absolute and relative array levels for open and closed wind tunnel sections. Acoustic array measurements were performed on wing noise from a 1:10.6 scaled Airbus A340 model in the open and closed test sections of the DNW-LLF wind tunnel. The purpose of these tests was to determine the acoustic effect of several wing devices that were intended to enhance the aerodynamic performance of the wing. The acoustic tests were done using a 4-m diameter out-of-flow microphone array in the open jet and a 1-m diameter wall array in the closed test section. The open jet results were used to systematically investigate the effect of DR and array size on the integrated sound levels. Moreover, since the same aircraft model was used in both test sections, the combined data base provided a unique opportunity to compare the array results for the open jet and closed test section quantitatively. Although in the end the array technique is intended for localization and quantification of different noise sources, in this study the integration method will be applied only to the complete model (or wing), in order to allow comparison to farfield microphone levels.

The structure of this article is as follows. In Section 2 the test set-up is described, followed by the data acquisition and processing procedures in Section 3. In Section 4 the integrated array spectra for both test sections are assessed in terms of absolute levels. Section 5 discusses the accuracy of relative sound levels, i.e. differences between configurations. The conclusions of this study are summarized in Section 6.

2. TEST SET-UP

The test campaigns in the open and closed test sections of the DNW-LLF were both performed using the 8x6 m^2 tunnel nozzle (Figure 1 and Figure 2). The same 1:10.6 scaled Airbus A340 model was used for both test campaigns. It had through-flow engine nacelles, winglets, and a vertical tail plane, but no horizontal tail plane and no landing gears. The wing span was 5.5 m and the length of the model was 5.9 m. The only model difference between the two test campaigns was related to the tripping of the slats. During the closed section tests (November 2003), where generally no tripping was applied, sometimes a narrowband tone occurred at the outer slat. This tone was considered to be due to the low Reynolds number and therefore not representative for the real aircraft. By tripping the slat the tone could be removed without affecting the aerodynamic performance of the wing or the broadband wing noise levels. Therefore in the subsequent open jet tests (January 2004) all slats were tripped.

The model was tested in take-off, landing, and approach configuration, and, as a background noise reference, also in the clean ('cruise') configuration. Measurements were done at wind speeds of 50, 60, and 70 m/s and angles of attack of about 3°, 5°, and 7°. The geometrical angles of attack were slightly lower in the closed section and slightly higher in the open jet, in order to compensate for the open jet effect and obtain the same lift. The model was tested in the baseline configuration and with several wing devices.

Acoustic measurements were done using a 4-m diameter out-of-flow microphone array in the open jet and a 1-m diameter wall array in the closed test section (Figure 3). The open jet array consisted of 140 LinearX M51 ½-inch microphones mounted in an acoustically open metal grid and was positioned below the left wing of the model, at a vertical distance of 7.6 m. The closed section array consisted of 128 LinearX M51 microphones flush-mounted in a plate on top of the tunnel floor (plate thickness a few centimetres), and was positioned below the right wing of the model, at a vertical distance of 3 m. Note that although three arrays were used in the closed section (to investigate directivity effects), in the present study only the central array is considered. Due to the different array diameters and distances, the (maximum) opening angle was θ_{OJ}=29° for the open jet array and θ_{CTS}=19° for the closed section array (Figure 4).

In order to measure the farfield directivity of the aircraft noise, a quarter-circle microphone boom (QCMB) with a radius of 7.3 m was used in the open jet, which could be traversed in flow direction (Figure 1). Although these farfield data are not analyzed in detail here, they will be used as a reference for the out-of-flow array levels.

3. DATA ACQUISITION AND PROCESSING

In both test campaigns data were acquired using the VIPER multi-channel data-acquisition system[18]. In the open jet the microphone signals were measured at a sample frequency of 102.4 kHz and a measurement time of 30 s. The acoustic data were processed using an FFT block size of 2048 with a Hanning window and an overlap of 50%, yielding 3000 averages and a narrowband frequency resolution of 50 Hz. In the closed test section the sample frequency was 122.88 kHz and the measurement time 20 s, leading to 1200 averages and a narrowband frequency resolution of 30 Hz (block size 4096). High-pass filters were used to suppress high-amplitude pressure fluctuations from the wind tunnel (at low frequencies), and thus to extend the dynamic range of the AD converter to low pressure amplitudes (at high frequencies). These 2nd order filters[18] reduced the pressure amplitudes for frequencies below 500 Hz (open jet) and 6 kHz (closed section). The levels presented here are corrected for the filter response. Prior to the measurements, all array microphones were calibrated at 1 kHz using a pistonphone. The frequency response of the individual open jet microphones was taken from calibration sheets provided by the manufacturer. The frequency-response of the individual closed section microphones (installed in the wall array) was taken from calibration measurements in an anechoic chamber. For low frequencies this amounted to the 6 dB correction for pressure doubling, but above 5 kHz the corrections deviated significantly from 6 dB (depending on frequency), probably due to details of the installation. No corrections were applied for microphone directivity, since these effects are considered to be small for the angles under consideration here. Phase matching of the microphones was checked prior to the tests using a cross-correlation analysis with a calibration source at known positions.

The array data were processed using conventional beamforming[19] to obtain the reconstructed source auto-powers A on a grid of scan locations in the plane of the model:

$$A = \frac{\sum_{m=1}^{N}\sum_{n=1}^{N} g_m^* C_{mn} g_n}{\sum_{m=1}^{N}\sum_{n=1}^{N} |g_m|^2 |g_n|^2} . \qquad (1)$$

In this equation, g is the steering vector for a given scan location, m and n are microphone indices, * indicates the complex conjugate, and C is the cross-spectral matrix containing the cross-powers between all pairs of microphones (for each narrowband frequency):

$$C_{mn}(f) = \tfrac{1}{2}\, p_m(f)\, p_n^*(f)\,. \tag{2}$$

From the reconstructed source auto-powers acoustic source maps in 1/3-octave bands were produced. The influence of uncorrelated noise was suppressed by discarding the main diagonal in the cross-spectral matrix (diagonal removal[1]), which corresponds to removing all m=n terms from the double summations in Equation (1). In the closed test section DR was also applied to remove pressure fluctuations from the turbulent wall boundary layer. It should be noted that DR only removes the uncorrelated part of the boundary layer noise. However, for the frequencies of interest the correlation lengths of the turbulent boundary layer noise are much smaller than the spacing between the microphones. The remaining wind tunnel noise was removed by subtracting the integrated background noise spectrum from the integrated wing noise spectrum (see Section 4.2). The effect of sound refraction by the open jet shear layer was corrected using a simplified Amiet method[20]. The scan grid, with a mesh size of 3 cm in the open jet and 2.5 cm in the closed section, was placed in the plane of the wings and rotated in accordance with the angle of attack. In order to reduce coherence loss effects and to increase the array resolution, spatial shading was applied to the microphone signals in the open jet. The first shading accounted for the variation of microphone density over the surface of the array. The second shading reduced the effective array radius r for increasing frequency according to r=B/f, with frequency f in kHz and B a measure for the frequency-dependent array size. For the open jet a standard value of B=6 m·kHz was used. No shading was applied to the closed section microphone signals, because array processing with variable effective array size indicated that coherence loss effects were small in this test section[11,21].

The source maps were further processed using a power integration method similar to the method described in Ref. 1, which is called the 'simplified method' in Ref. 2. This technique sums the source powers in (part of) the measured source map, and corrects the results with a scaling factor obtained by performing a simulation for a monopole source at the centre of the integration region:

$$P_{exp} = \sum_{h=1}^{H} A_{h,exp} \times \frac{P_{sim}}{\sum_{h=1}^{H} A_{h,sim}}\,. \tag{3}$$

In this equation, P_{exp} is the integrated source power, P_{sim} is the source power of the simulated source, A_h are the simulated or experimental beamforming results, and h is the scan grid index. In order to prevent contributions from negative 'source powers' in the case of DR, the scan levels A_h that were negative or more than 12 dB below the peak level (in the simulated or measured source map) were set to zero. It should be noted that, because the scaling factor in equation (3) is determined using a single monopole source at the centre of the scan grid, the simplified integration method is only valid if the variation in array resolution (or beamwidth) over the integration region is small. For the present study this was verified by simulations of an extended line source and by using multiple integration regions with reduced size (see also Section 4.3). In order to suppress contributions from spurious side lobes, the integration contours for the open jet and closed section were fitted around the wings (Figure 5). For the open jet both wings were integrated to allow comparison of the integrated levels to absolute sound levels in the farfield. For the closed test section only the right wing

was integrated because of the oblique view angle to the left wing (Figure 4), which led to a significantly lower resolution.

To enable a good comparison between the integrated array levels and the array auto-powers, the 'Average Array Auto-Powers' (AAAP) were calculated. These were obtained by averaging the auto-powers of all array microphones, using the same (frequency-dependent) microphone weights as applied during the beamforming (see above). The AAAP were also compared to the sound levels measured at the quarter-circle farfield microphone boom. In order to obtain approximately the same directivity, the average level of the farfield positions opposite of the array was used (Figure 6). Three decibels were added to the integrated array spectra for the closed section to account for the second wing. Finally, all farfield and integrated array spectra were normalized to the same reference distance (including a correction for atmospheric absorption) to allow direct comparison of the levels. The source maps and spectra are presented in 1/3-octave bands at model scale frequencies, without A-weighting.

4. ABSOLUTE SOUND LEVELS

In this section the integrated array spectra are assessed in terms of absolute sound levels. In Section 4.1 the source maps for both test sections are compared. In Section 4.2 the absolute integrated levels are compared to the sound level measured by the farfield microphones in the open jet. In Section 4.3 the differences between the array spectra and farfield levels are further analyzed.

4.1 Source maps

Figure 7 shows the source maps for the landing configuration, for the closed test section and the open jet. The left wing source maps of the open jet are mirrored to allow easier comparison to the closed test section. For the open jet, the results with and without diagonal removal are shown. It can be seen that DR drastically improves the results by eliminating the high noise floor in the source maps. This indicates that the main diagonal of the cross-spectral matrix contains a significant amount of uncorrelated 'noise' which is not present in the off-diagonal terms. Since the signal-to-noise ratio is good in this frequency range (see below), these uncorrelated signals in the main diagonal are not due to wind tunnel background noise, but due to noise from the model which has lost its phase relationship as a result of coherence loss[11,22].

For the closed test section only the results with DR are shown, since in this case the main diagonal was contaminated by tunnel wall boundary layer fluctuations, again leading to source maps with a high noise floor. Comparison between the closed section and open jet results shows that, although the array resolution is different, the source characteristics are quite consistent: at low frequencies the dominant noise sources are located close to the inner engine and at the trailing edge flaps, while for increasing frequency the outer slat becomes more important. In terms of resolution the open jet array performs better than the closed section array at low frequencies, but worse at high frequencies. Around 4-5 kHz the resolution is similar, because at that frequency the effective opening angle (Figure 4) is approximately the same for both arrays (note that with B=6 m·kHz the effective radius of the open jet array at 4 kHz is 1.5 m).

4.2 Integrated spectra

The source maps were quantified using the power integration method described in Section 3. Note that for the open jet both wings were integrated, to allow comparison to absolute sound levels in the farfield (Figure 5). Before comparing the integrated levels to the farfield spectra, it is useful to look at the signal-to-noise ratio (SNR) for the different methods (Figure 8). The SNR was defined as the difference in noise level between the landing and clean (or 'cruise')

configuration, which was used as a background noise reference. For the farfield microphones (AAAP and QCMB, see Figure 6), the SNR increases from about 2 dB at low frequencies to 12 dB at high frequencies. For the integrated open jet array spectra with DR the SNR is generally much higher, because the array focuses on the wing noise and thus reduces background noise from the wind tunnel. However, when DR is *not* applied, the SNR reduces to the AAAP level above 2.5 kHz, due to the high noise floor in the source maps. The SNR for the closed test section is significantly lower than in the open jet (with DR). At low frequencies this is due to the influence of extraneous noise sources in the wind tunnel (e.g. the sting), which influence the integrated wing noise as a result of the limited array resolution. At high frequencies the relatively low SNR is due to the fact that the (leading edge) source region occupies only a small part of the (full wing) integration region. As a result of the large integration area the low noise floor in the source map adds up to a significant level. Therefore, the SNR could be improved by using a smaller integration area around the sources or by increasing the spot size by reducing the effective array size (and thus resolution).

Figure 9 compares the integrated spectra for the different methods. All spectra were corrected for background noise (see SNR in Figure 8). The farfield spectra QCMB and AAAP are quite consistent, except at the low frequencies where the SNR is relatively low. In order to obtain the most direct comparison, in the remainder of this article the AAAP will be used as a reference for the integrated array spectra. The integrated open jet spectra are cut off at 16 kHz because at higher frequencies side lobes dominate the source maps, due to the reduced array size (and thus smaller number of microphones). When DR is not applied in the open jet, the integrated levels are increased due to the high noise floor in the source maps (Figure 7). As mentioned before, this noise floor is due to noise from the model which has lost its phase relationship as a result of coherence loss. So even though the SNR is quite high, the integration method without DR is not suitable for quantification of different source regions on the model[11]. When DR is applied, the integrated levels are close to the AAAP at low frequencies, but significantly lower for increasing frequency. The spectrum for the closed test section is relatively close to the open jet AAAP over the whole frequency range (within 3 dB). Note that the CTS spectrum starts at 1.6 kHz because at lower frequencies the resolution is too low for reliable wing noise integration.

4.3 Difference between array spectra and farfield levels

Several possible explanations for the differences between the integrated array spectra and the open jet Average Array Auto-Powers (AAAP) were examined. First, systematical errors may occur due to simplifications used in the integration method (e.g. the assumption of constant beamwidth over the integration region). Such errors were quantified by performing simulations for a line source at the wing leading edge, and comparing the experimental deviation from the open jet AAAP to the simulated deviation (Figure 10). For the closed test section (CTS) the simulated deviation is always smaller than 1 dB, but for the open jet a difference of almost 6 dB occurs at 16 kHz. Additional simulations (not shown here) indicated that this deviation is not caused by negative side lobes (due to DR) that reduce the level of adjacent sources on the leading edge. Possible errors due to the assumption of a constant beamwidth were investigated by using multiple integration regions with reduced size, and were also found to be small. Rather, the difference turned out to be due to side lobes which are *inside* the integration contour for the simulated point source used to calculate the scaling factors, but are *outside* the integration contour in the actual measurement. This analysis shows that systematical errors may be present when significant side lobes occur, such as in the open jet at high frequencies (these errors could be reduced by increasing the number of microphones or integrating less than 12 dB below peak level). However, for both test sections these errors do not (fully) explain the experimentally observed differences between integrated spectra and AAAP.

For the open jet, a probable cause for the reduced integrated levels is coherence loss[11,22]. As mentioned in Section 1, coherence loss effects increase with distance between the

microphones. Therefore, the effect of varying the array size parameter *B* was investigated for the open jet. The source maps in Figure 11 show that the resolution increases with increasing array size. However, at high frequencies coherence loss between distant microphones results in a high noise floor. When the array is kept smaller (*B*=3) the noise floor is suppressed, but at high frequencies side lobes start to dominate the source maps due to the small number of microphones. These observations are reflected in Figure 12, which shows the deviation from the AAAP (the AAAP were calculated for each array size, although these showed very little variation). For low frequencies the four lines coincide because all array microphones are used in all cases. For intermediate frequencies, the integrated level decreases with increasing array size, due to coherence loss. For the highest frequencies, the integrated levels for the largest array increase due to the high noise floor. All in all the best compromise seems to be achieved at *B*=6, which was used as the standard value. Besides the distance between the microphones, coherence loss effects are also expected to increase with wind speed, due to the higher turbulence levels in the open jet shear layer. This is confirmed in Figure 13, which shows that the deviation from the AAAP increases with wind speed. Thus, for the open jet the difference between integrated array spectra and AAAP can be explained mainly by coherence loss and to a lesser extent by systematic errors.

The possible presence of coherence loss in the closed test section was investigated by reducing the array size and comparing the integrated array levels to those from the full array. If coherence loss were present, the integrated levels should increase with decreasing array size, similar to the open jet (Figure 12). However, when the outer one, two or three microphone rings were removed in the array processing, the integrated spectra remained practically the same (within 0.5 dB). Thus, similar to Ref. 11, coherence loss does not seem to be significant in the closed test section, and cannot explain the (relatively small) experimentally observed differences between integrated array spectra and AAAP (Figure 10).

Another reason for these differences could be directivity: whereas the AAAP contain noise contributions from both wings under different angles, the integrated CTS array spectrum contains the noise from one wing only (Figure 4). Although 3 dB was added to the CTS spectrum to account for the second wing, a strong lateral directivity (i.e. perpendicular to the flow direction) of the wing noise could cause a difference between the integrated CTS spectrum and the AAAP from the open jet. This directivity effect was quantified by calculating the left and right wing spectra separately for the open jet test. The resulting spectra differed less than 1 dB, indicating that the wing noise has no strong lateral directivity for the angles considered here. From the wing noise footprints obtained from the quarter-circle microphone boom (not shown here) it can be concluded that also the *polar* directivity (i.e. in the flow direction) is small in the direction of the arrays.

Another possible explanation for the difference between the CTS spectrum and the open jet AAAP could be microphone installation effects. The free-field microphones in the open jet array were installed in a non-reflecting, acoustically open metal grid, while the CTS microphones were flush-mounted in a wall array. As mentioned in Section 3, the frequency-response of the installed wall array microphones was determined in an anechoic chamber, outside the wind tunnel, and was found to deviate significantly from the 6 dB correction for pressure doubling at frequencies higher than 5 kHz. It could be that small details of the installation slightly affect the response of the array microphones. This may be checked by an *in-situ* array calibration.

Finally, the difference between integrated array levels in the CTS and the AAAP in the open jet could be due to a difference in the flow parameters. As mentioned in Section 2, the geometrical angle of attack in the closed test section was slightly lower than in the open jet, in order to obtain the same lift coefficient. However, equal lift does not necessarily mean that the wing flow parameters are the same. Aerodynamic measurements on wind turbine airfoils in open and closed wind tunnel sections have indicated that *for equal lift* the boundary layer transition from laminar to turbulent occurs more upstream in the open jet than in the closed test section[23]. Although the ratio of wing chord over tunnel dimension is much smaller

in the present DNW tests, different transition or separation locations may significantly affect the aerodynamic noise produced by the high-lift configurations studied here. Such effects might explain the differences in source characteristics between the open jet and the closed test section (Figure 7). This issue will be further discussed in Section 5.

5. RELATIVE SOUND LEVELS

Whereas in the previous section the accuracy of the *absolute* sound levels was assessed, the present section deals with the accuracy of *relative* sound levels. With relative sound levels the noise differences between different configurations are meant, often the most important quantity in aeroacoustic tests. Since the tested wing devices only had a small effect on the wing noise (generally below 1 dB), they were not very suitable for assessing relative sound levels. Therefore, in this section wing noise differences due to variation in wind speed, angle-of-attack, and flap angle will be used to assess the accuracy of the relative integrated spectra for the open and closed test section, by comparison to the open jet AAAP.

In order to investigate the speed dependence of the wing noise, normalized sound levels were plotted as a function of Strouhal number $St=f \cdot L/U$, where f is frequency, U is wind speed, and L is a length scale for which here a constant value of 1 cm was chosen. The sound levels were normalized as $SPL-10 \cdot x \cdot log(U)$, where x indicates the dependence of the wing noise on the flow speed ($p^2 \sim U^x$). For the AAAP, which are regarded to represent the true wing noise levels, the best data collapse is obtained for x=5 (Figure 14). However, if the same scaling is applied to the integrated array spectra for the open jet, significant scatter occurs at high St. This is due to the fact that the deviation of the integrated array levels from the AAAP (due to coherence loss) increases with wind speed (Figure 13). Thus, in the open jet one should be careful to compare integrated array spectra for different wind speeds, because this may lead to too low speed exponents. For example, to collapse the high frequencies of the integrated open jet spectra, a value of 1 should be used for x, which is much lower than the actual value of 5. For the integrated array spectra in the closed test section also a small amount of scatter occurs at high St (Figure 14), which may indicate that some coherence loss occurs here as well, although reducing the array size did not increase the integrated levels (see previous section).

Next, the effect of aircraft angle-of-attack on wing noise was examined for the open jet and the closed test section. Figure 15 shows the source maps at 5 kHz, where the array performance is similar for both test sections. For the lower angles of attack the source characteristics are quite consistent: at 3° the middle wing is most important, whereas at 5° the outer wing becomes dominant. At 7° a dominant noise source appears in the open jet close to the outboard engine, which is not present in the closed section. As argued in the previous section, this difference in source characteristics is most probably not due to directivity effects, but due to different flow conditions caused by the different geometrical angle-of-attack. The "delta spectra" for the three angles of attack are shown in Figure 16 for the three different methods: the AAAP and integrated array spectra for the open jet, and the integrated array spectra for the closed test section. The CTS spectra for the highest frequencies ($\geq$ 10 kHz) were calculated using a reduced array size to improve the SNR (see Section 4.2). Figure 16 shows that the integrated array spectra for the open jet agree to the AAAP within 0.5 dB over the whole frequency range, for both changes in angle-of-attack. Thus, the power integration method is very reliable in terms of relative noise levels. Moreover, it is seen that the delta spectra from the closed section also agree within 1 dB, despite the small differences in source characteristics mentioned above. This illustrates that when the flow conditions - and therefore the noise source characteristics - are similar, the phased array results for the open and closed section are very consistent.

Finally, Figure 17 shows the effect of varying flap angle for both test sections, again in terms of delta spectra. The source characteristics seem to be fairly similar: for increasing flap angle the dominant noise source at the middle wing decreases, while the source just

outside the outboard wing increases in strength. If we compare the open jet AAAP to the integrated array spectra in the open jet (Figure 18), the results are consistent within 0.5 dB, which confirms the reliability of the array method to determine relative noise levels (i.e. differences between configurations). However, if we compare relative spectra from the open jet to those from the closed test section (Figure 19), large differences occur. Whereas the CTS spectra consistently show an increase in noise each time the flap angle is increased, the open jet spectrum decreases when the flap angle changes from 32° to 35°. This difference between open and closed test section cannot be explained by an inaccuracy in the integration method, since the integrated array spectra were shown to be accurate within 0.5 dB in terms of relative noise levels. In the previous section it was already mentioned that differences in directivity due to the different array set-ups in both sections are also small. Apparently, different flow conditions in the open jet and closed test section result in relatively large differences in wing noise. It was checked if this might be caused by the fact that the slats were tripped in the open jet while they were not tripped in the closed section (see Section 2). However, comparison of closed section measurements with and without trips showed that these only removed tonal noise and did not affect broadband noise levels significantly. This suggests that in some cases the flow conditions in the open jet and closed test section are not identical, even though the produced lift may be the same.

6. CONCLUSIONS

The reliability of the phased array technique for quantifying airframe noise was assessed in the DNW-LLF open and closed wind tunnel sections. Acoustic measurements were performed on wing noise from a 1:10.6 scaled Airbus A340 model, using a 4-m diameter out-of-flow microphone array in the open jet and a 1-m diameter wall array in the closed test section. Since the same aircraft model was used in both test sections, the array results for the open jet and closed test section could be compared quantitatively. The spectra measured by farfield microphones in the open jet were used as a reference for the absolute sound level.

In both test sections diagonal removal was applied to obtain meaningful array results. In terms of resolution the array performance was similar for both sections around 4-5 kHz. For lower frequencies the open jet array performed better, for higher frequencies the closed section array. Apart from the differences in array resolution, the source characteristics were generally similar for both test sections.

The results for the open jet show that, although the *absolute* integrated array level can be too low by more than 10 dB due to coherence loss, the *relative* sound levels determined with the array (i.e. differences between configurations) are accurate within 0.5 dB. Since the amount of coherence loss depends on wind speed, one should be careful to compare integrated spectra for different wind speeds.

The difference between the absolute array levels in the closed test section and the farfield levels in the open jet is smaller than 3 dB for all frequencies. The *relative* array levels in the closed test section agree with the open jet within 1 dB, provided that the flow conditions - and therefore the noise source characteristics - are similar. In some cases larger differences between the two test sections occur, especially at high-lift conditions. These differences are most likely due to slightly different flow conditions in the open jet and closed test section, even though the angle-of-attack is adjusted such that the produced lift is the same.

ACKNOWLEDGMENTS

The authors would like to thank the colleagues from DLR, Airbus, and DNW for their valuable contributions to the definition of the tests and the interpretation of the results. The comments from A. Hirschberg (University of Twente) during this study are highly appreciated. For this investigation use was made of wind tunnel results from the AWIATOR project, which was sponsored by the European Commission.

FIGURES

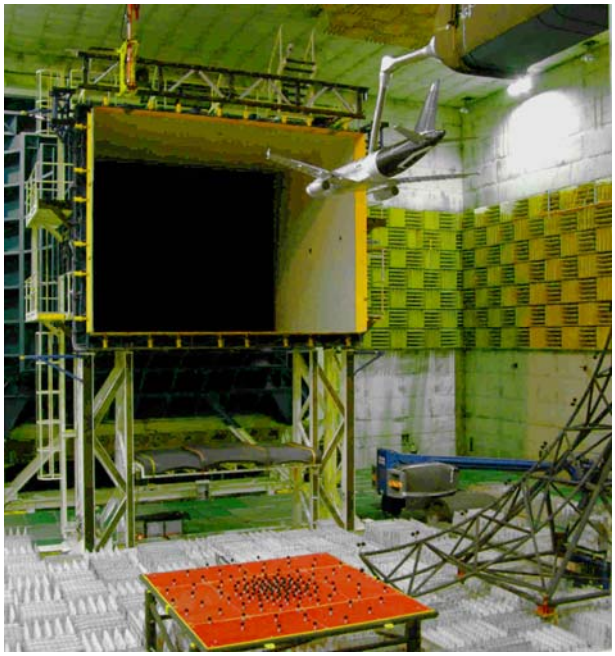

Figure 1: Test set-up in DNW open jet, with out-of-flow microphone array (in red) and farfield quarter-circle microphone boom.

Figure 2: Test set-up in DNW closed test section, with wall arrays on the tunnel floor.

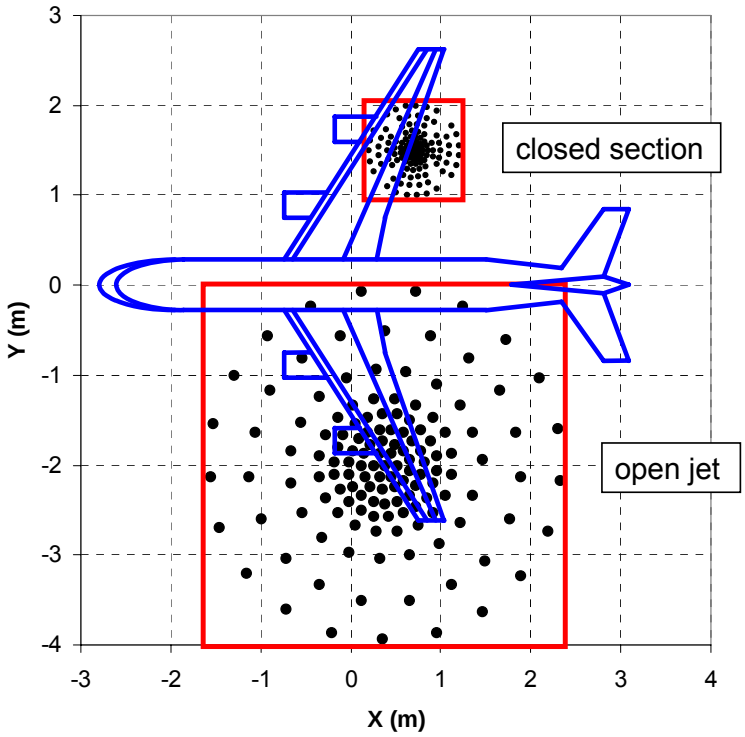

Figure 3: Top view of array positions for closed test section and open jet.

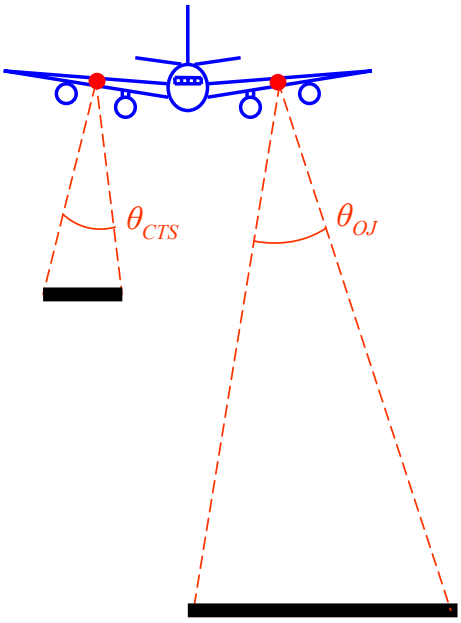

Figure 4: Front view of array positions for closed test section and open jet.

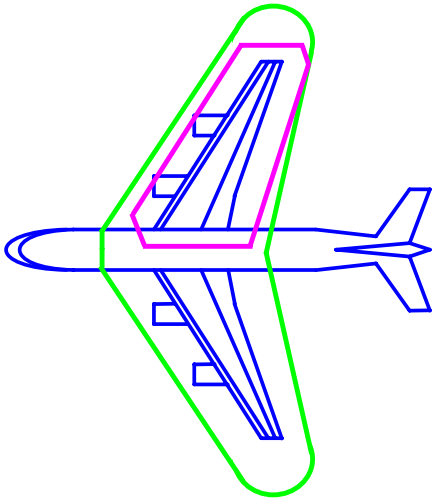

Figure 5: Integration contours for open jet (green) and closed test section (pink).

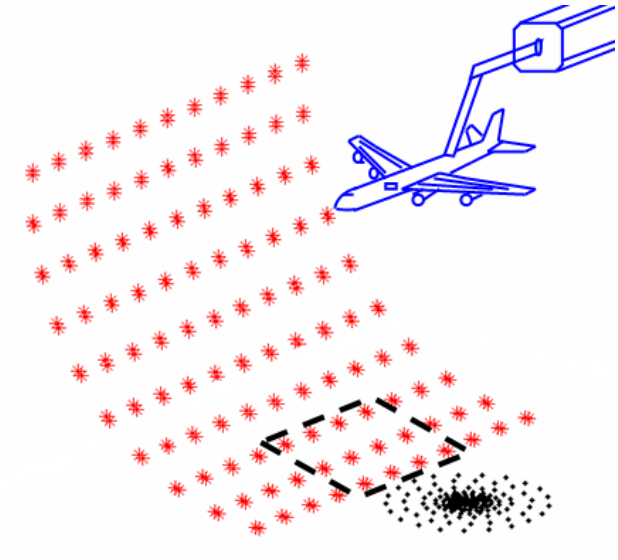

Figure 6: The dashed rectangle indicates the farfield microphone positions that were used as a reference for the out-of-flow array levels.

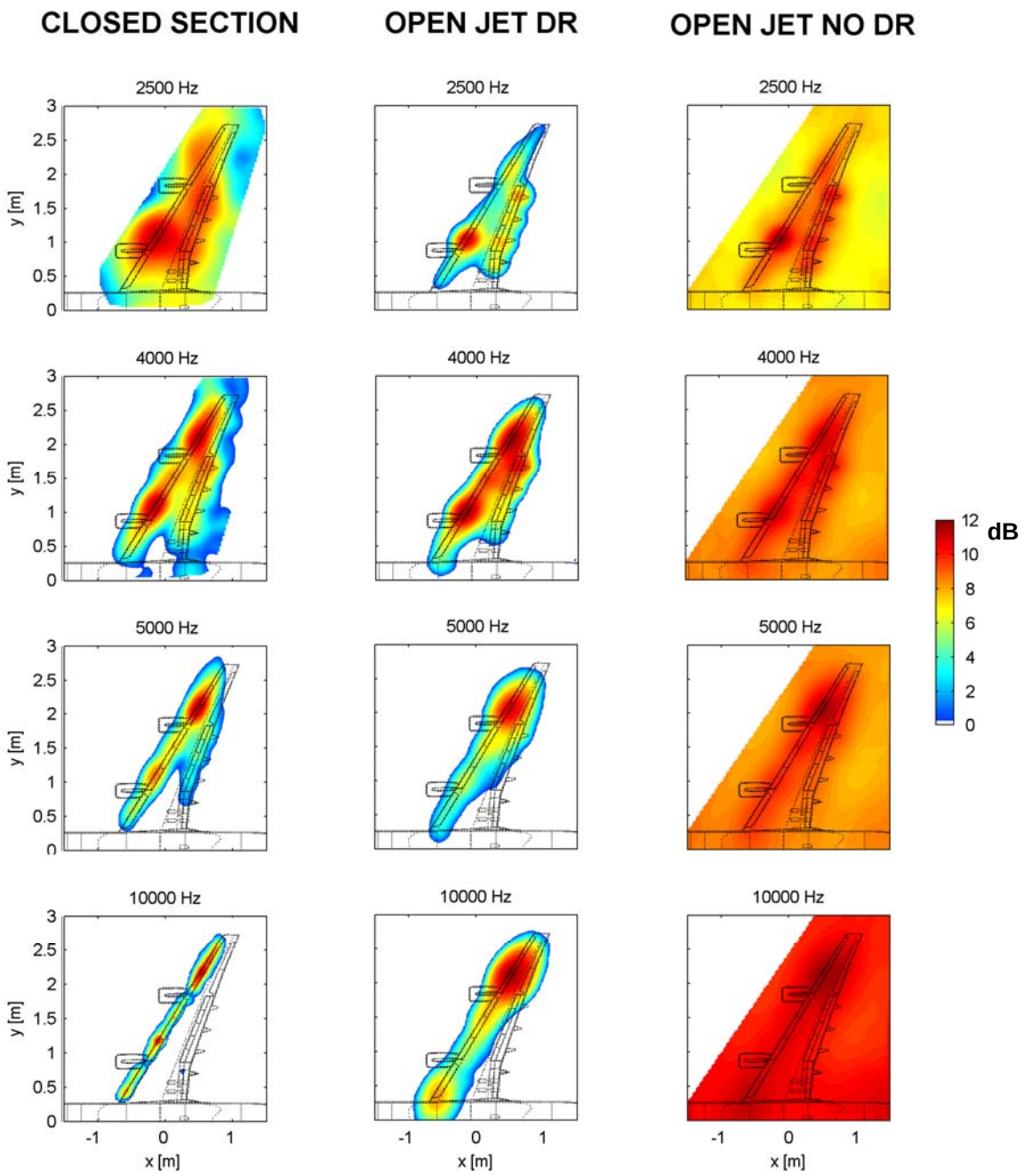

Figure 7: Source maps for landing configuration at U*=60 m/s and* α*=5°. Results are shown for the closed test section (with DR) and the open jet (with and without DR). The range of the colour scale is always 12 dB, the maximum level is adjusted for each individual plot.*

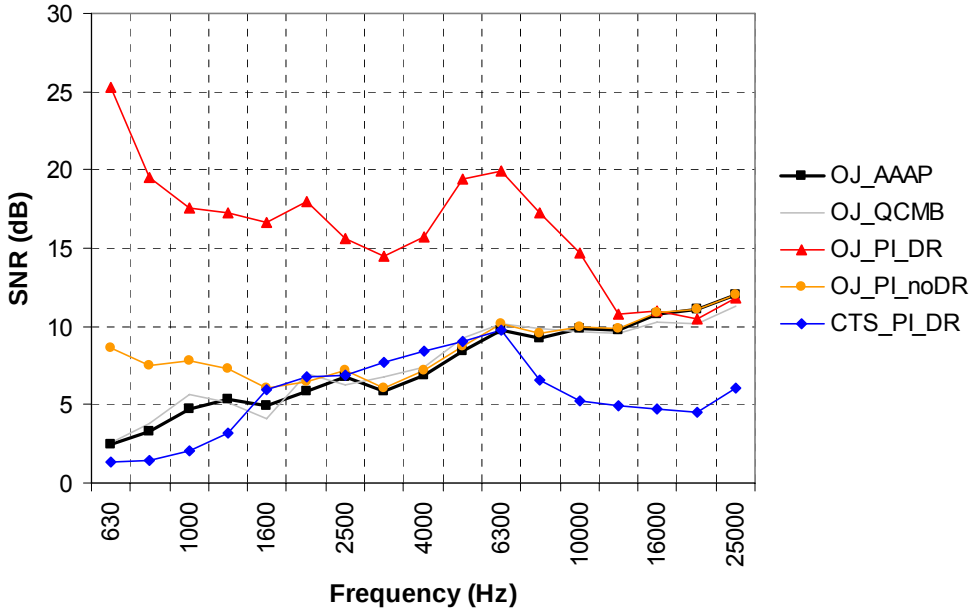

Figure 8: Signal-to-noise ratio at U=*60 m/s and* α=*5°, for different methods in open jet (OJ) and closed test section (CTS): average array auto-powers (AAAP), quarter-circle microphone boom (QCMB), and power integration (PI) with and without diagonal removal (DR).*

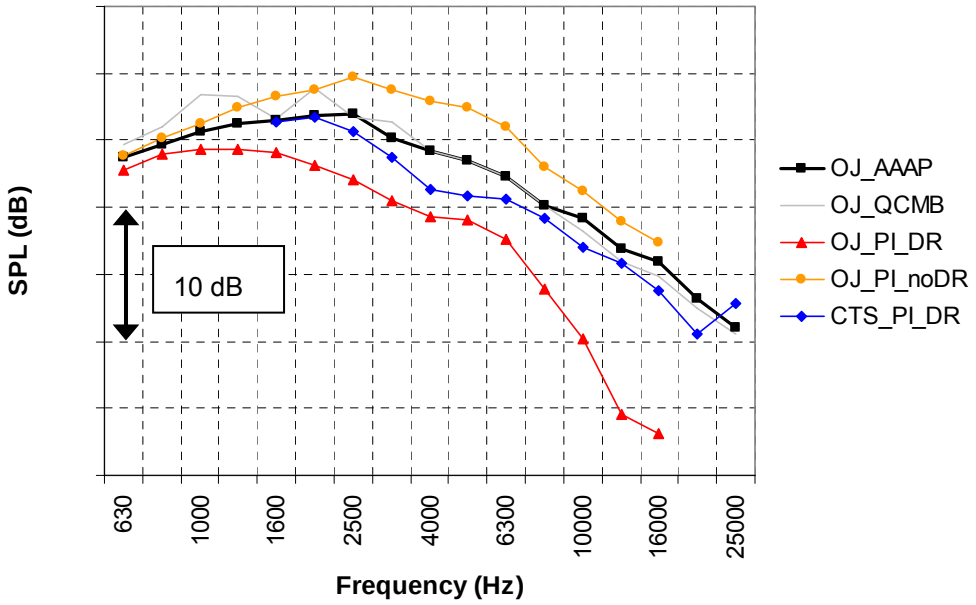

Figure 9: Absolute sound levels for landing configuration at U=*60 m/s and* α=*5°, using different methods. Same legend as in Figure 8.*

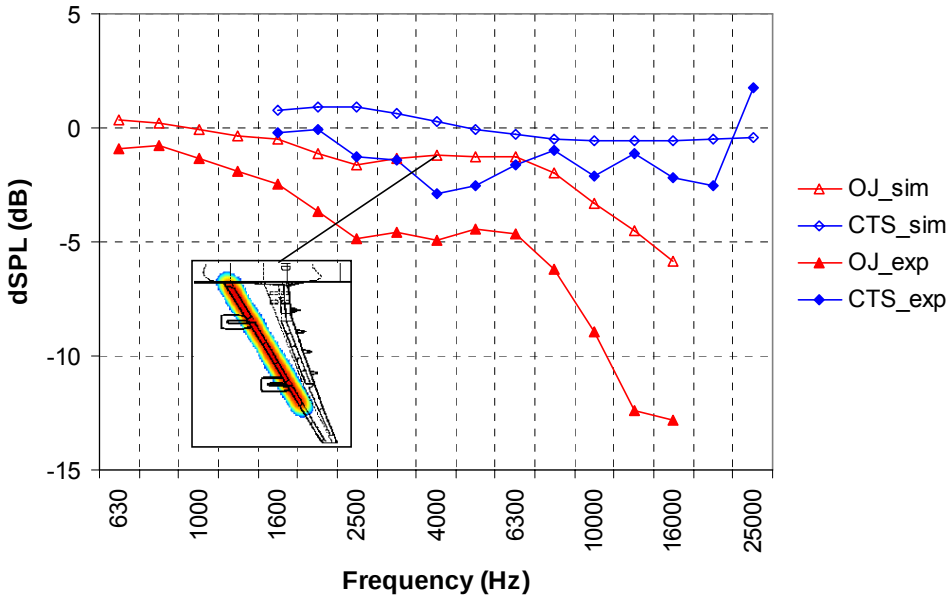

Figure 10: Deviation of integrated array spectra (with DR) from open jet AAAP, for measured wing noise and for simulated line source at wing leading edge.

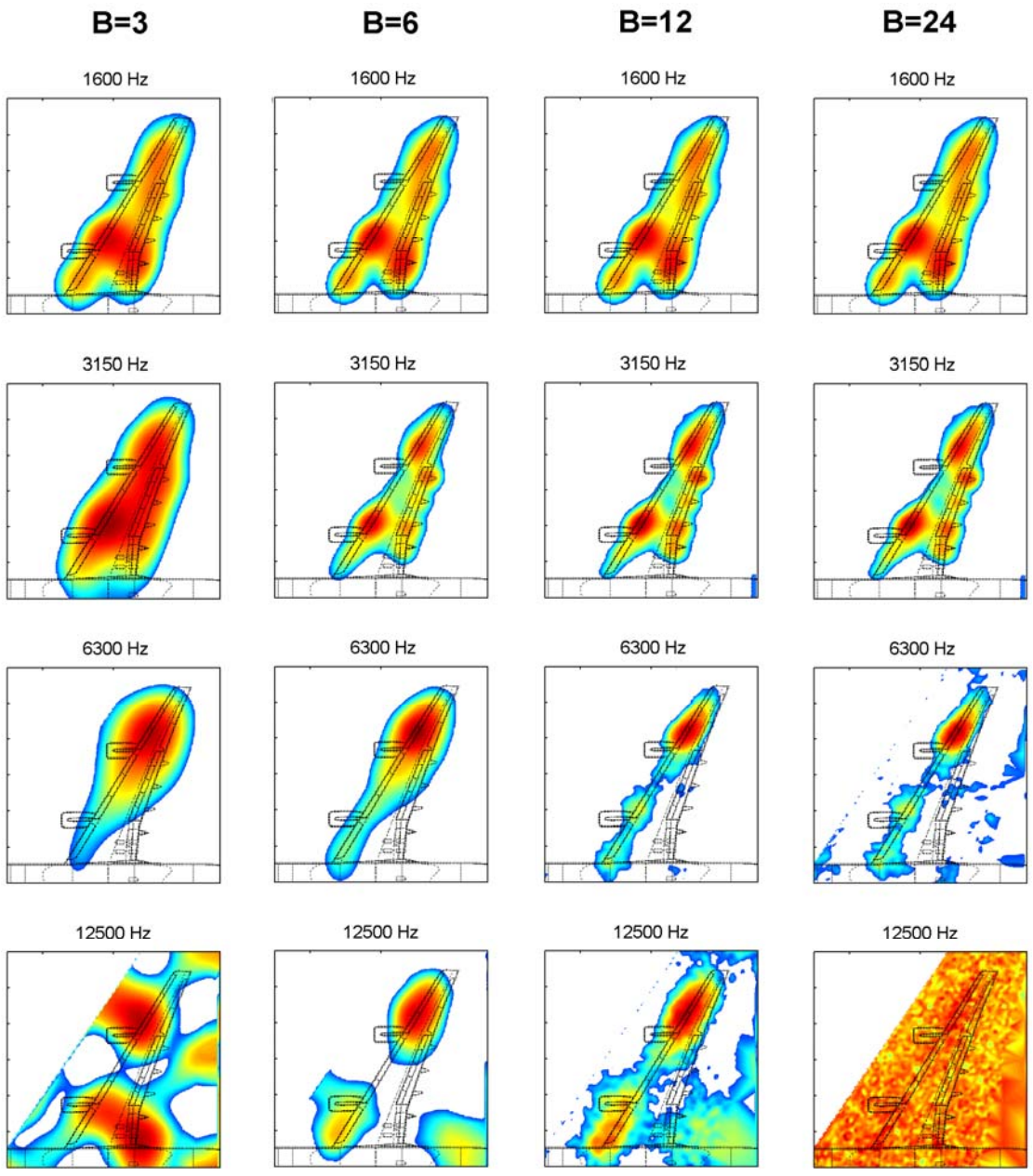

Figure 11: Open jet source maps for landing configuration at U=*60 m/s and* α=*5°, for different values of array size parameter* B.

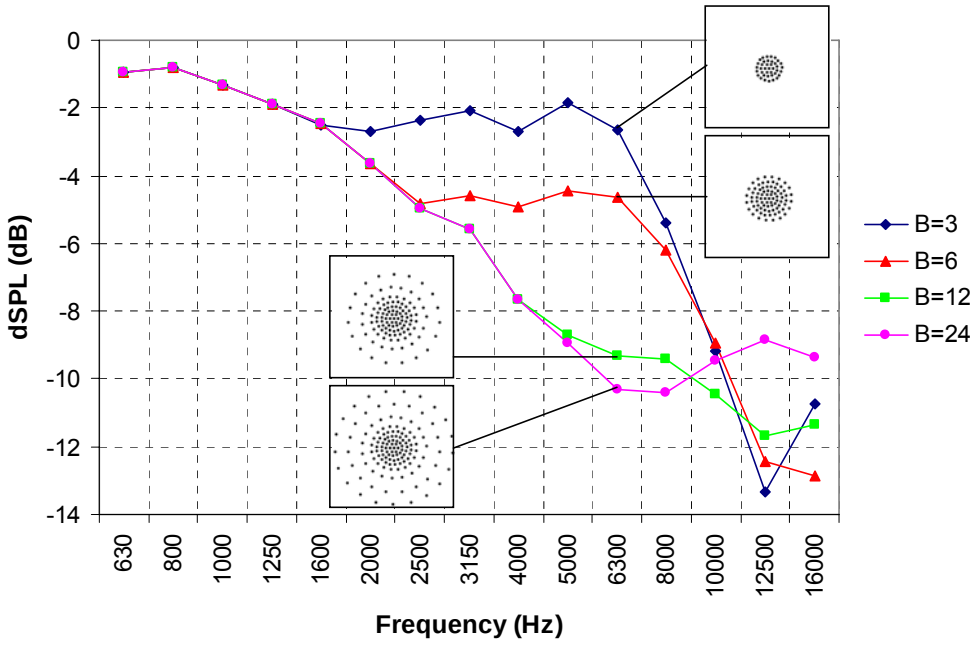

Figure 12: Deviation of integrated open jet array spectra (with DR) from AAAP, for different values of the array size parameter B*. The array size at 6.3 kHz is indicated in the figure. Landing configuration at* U*=60 m/s and* α*=5°.*

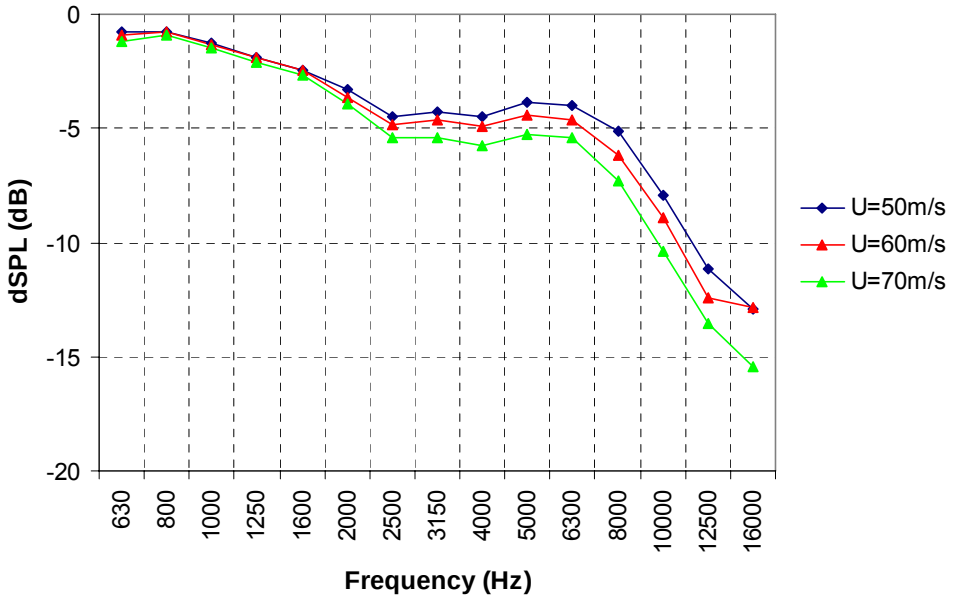

Figure 13: Deviation of integrated open jet array spectra (with DR) from AAAP, for different wind speeds. Landing configuration at α*=5°.*

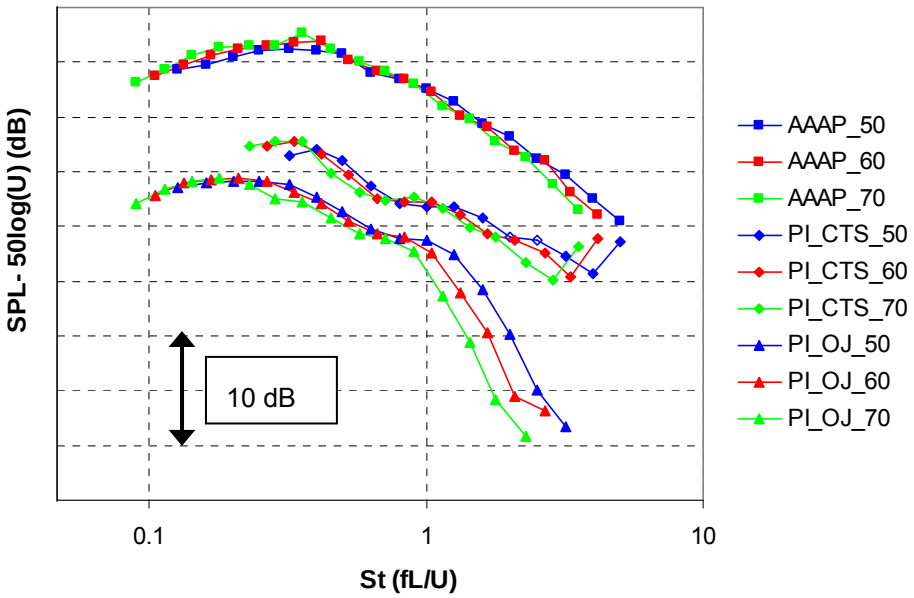

Figure 14: Normalized spectra at three wind speeds (50, 60, and 70 m/s) for the AAAP and for the integrated array spectra (with DR) in the open jet and the closed test section. Landing configuration at α=5°. The two open markers in the PI_CTS_50 spectrum indicate that a narrowband tone was removed from the spectrum.

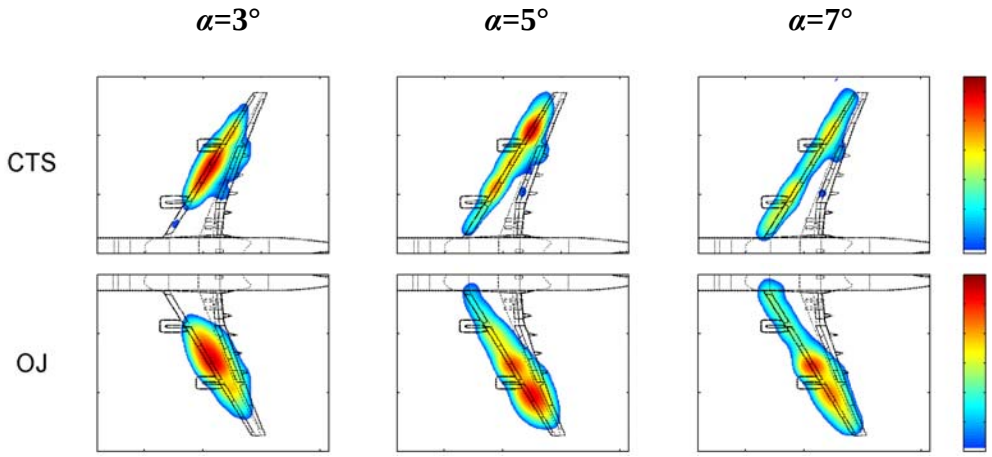

Figure 15: Effect of angle-of-attack on the source characteristics in the closed test section and open jet (5 kHz), for the approach configuration at U=60 m/s. The maximum level of the 12 dB colour scale is the same within both rows.

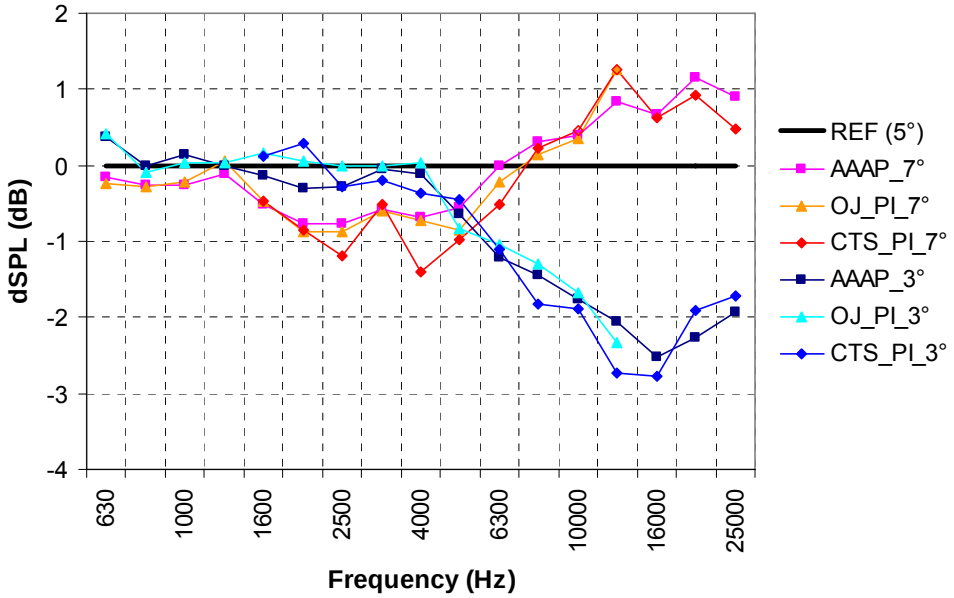

Figure 16: Effect of angle-of-attack on wing noise for the approach configuration at U=*60 m/s. Shown are the open jet AAAP and the integrated array spectra for the open jet and the closed test section. All spectra are referenced to the respective spectrum at 5°.*

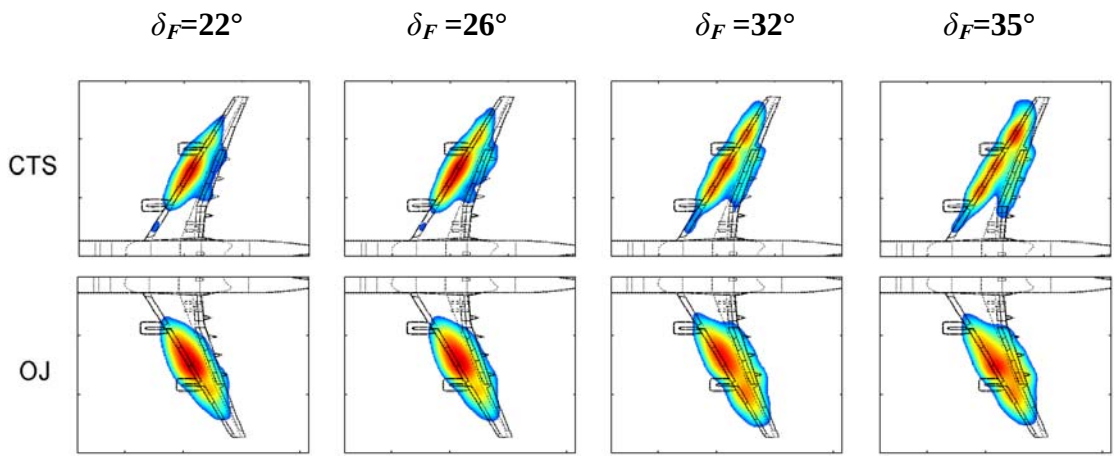

Figure 17: Effect of flap angle on the source characteristics in the closed test section and open jet (5 kHz) at U=*60 m/s and* α=*3°. The maximum level of the 12 dB colour scale is the same within both rows.*

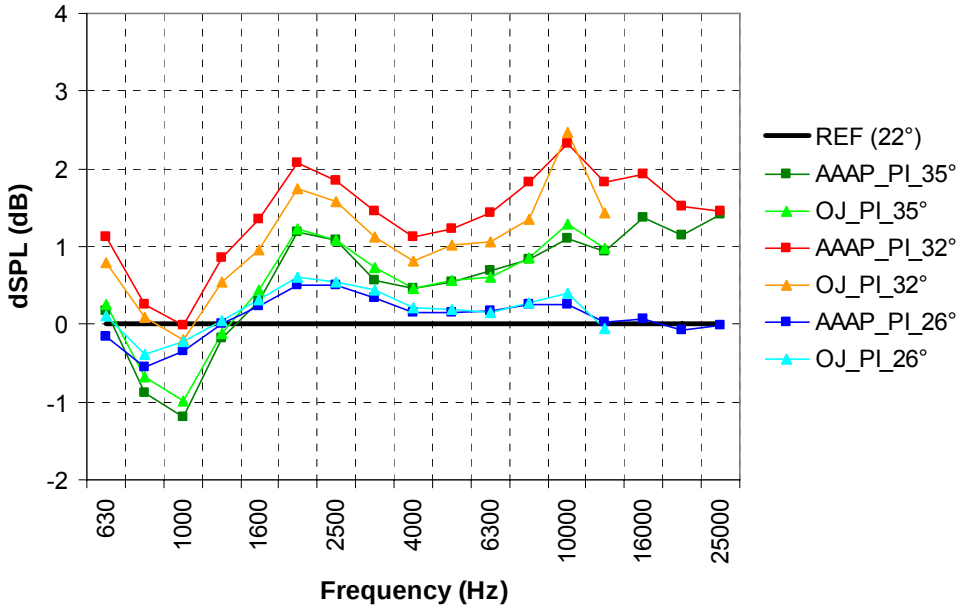

Figure 18: Effect of flap angle on wing noise at U=*60 m/s and* α=*3°. Shown are the open jet AAAP and the integrated array spectra for the open jet. All spectra are referenced to the respective spectrum at a flap angle of 22°.*

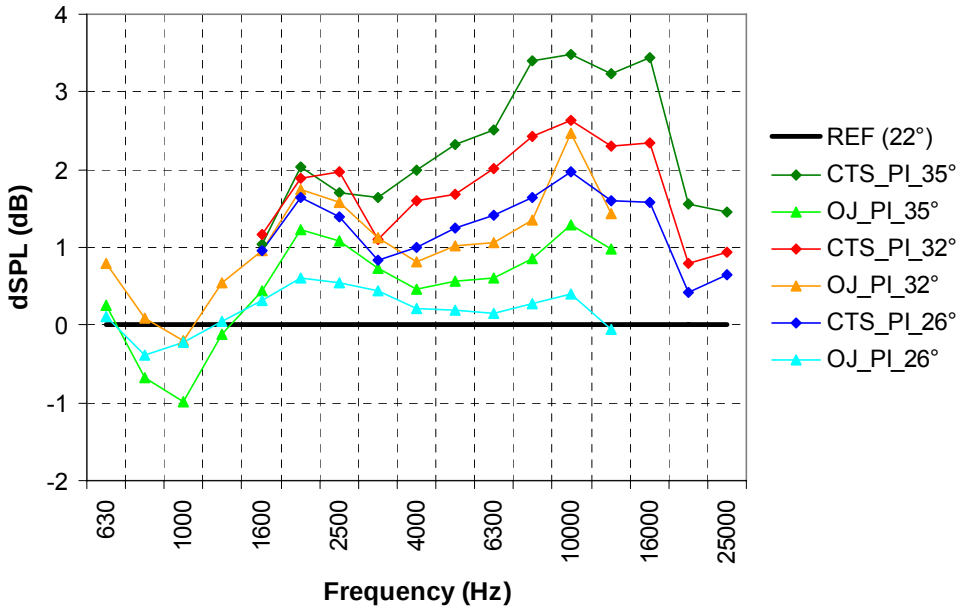

Figure 19: Effect of flap angle on wing noise at U=*60 m/s and* α=*3°. Shown are the integrated array spectra for the open jet and the closed test section. All spectra are referenced to the respective spectrum at a flap angle of 22°.*

REFERENCES

1. Mosher, M., "Phased arrays for aeroacoustic testing - Theoretical development", AIAA paper 96-1713, 1996.
2. Brooks, T.F., and Humphreys, W.M., "Effect of directional array size on the measurement of airframe noise components", AIAA paper 99-1958, 1999.
3. Dougherty, R.P., "Source Location with Sparse Acoustic Arrays; Interference Cancellation", Presented at the First CEAS-ASC Workshop: Wind Tunnel Testing in Aeroacoustics, DNW, 5-6 November 1997.
4. Soderman, P.T., Kafyeke, F., Burnside, N., Chandrasekharan, R., Jaeger, S., Boudreau, J., "Airframe Noise Study of a CRJ-700 Aircraft Model in the NASA Ames 7- by 10-foot Wind Tunnel No. 1", AIAA paper 2002-2406, 2002.
5. Blacodon, D., and Elias, G., "Level estimation of extended acoustic sources using an array of microphones", AIAA paper 2003-3199, 2003.
6. Sijtsma, P., and Stoker, R.W., "Determination of Absolute Contributions of Aircraft Noise Components using Fly-Over Array Measurements", AIAA paper 2004-2958, 2004.
7. Oerlemans, S., and Sijtsma, P., "Determination of Absolute Levels from Phased Array Measurements Using Spatial Source Coherence", AIAA paper 2002-2464, 2002.
8. Mendoza, J.M., Brooks, T.F., and Humphreys, W.M., "An aeroacoustic study of a leading edge slat configuration", International Journal of Aeroacoustics, Vol. 1, Nr. 3, 2002.
9. Hutcheson, F.V., and Brooks, T.F., "Effects of Angle of Attack and Velocity on Trailing Edge Noise", AIAA paper 2004-1031, 2004.
10. Oerlemans, S., and Migliore, P., "Aeroacoustic Wind Tunnel Tests of Wind Turbine Airfoils", AIAA paper 2004-3042, 2004.
11. Oerlemans, S., and Sijtsma, P., "Acoustic array measurements of a 1:10.6 scaled Airbus A340 model", AIAA paper 2004-2924, 2004.
12. Brooks, T.F. and Humphreys, W.M., "A deconvolution approach for the mapping of acoustic sources (DAMAS) determined from phased microphone arrays", AIAA paper 2004-2954, 2004.
13. Dougherty, R.P., "Extensions of DAMAS and benefits and limitations of deconvolution in beamforming", AIAA paper 2005-2961, 2005.
14. Brooks, T.F. and Humphreys, W.M., "Three-dimensional application of DAMAS methodology for aeroacoustic noise source definition", AIAA paper 2005-2960, 2005.
15. Brooks, T.F. and Humphreys, W.M., "Extension of DAMAS phased array processing for spatial coherence determination (DAMAS-C)", AIAA paper 2006-2654, 2006.
16. Ravetta, P.A., Burdisso, R.A., and Ng, W.F., "Noise source localization and optimization of phased array results (LORE)", AIAA paper 2006-2713, 2006.
17. Ehrenfried, K. and Koop, L., "A comparison of iterative deconvolution algorithms for the mapping of acoustic sources", AIAA paper 2006-2711, 2006.
18. Holthusen, H. and Smit, H., "A new data-acquisition system for microphone array measurements in wind tunnels", AIAA paper 2001-2169, 2001.
19. Johnson, D.H., and Dudgeon, D.E., "Array Signal Processing", Prentice Hall, 1993.
20. Amiet, R.K., "Refraction of Sound by a Shear Layer", Journal of Sound and Vibration, Vol. 58, No. 2, pp. 467-482, 1978.
21. Broersma, L., "Acoustic Array Measurements - Airframe Noise and Wind Turbine Noise", Master's Thesis, Twente University, January 2006.
22. Dougherty, R.P., "Turbulent decorrelation of aeroacoustic phased arrays: lessons from atmospheric science and astronomy", AIAA paper 2003-3200, 2003.
23. Herrig, A., Würz, W., Lutz, T., Braun, K., Krämer, E., Oerlemans, S., "Trailing-edge noise measurements of wind turbine airfoils in open and closed test section wind tunnels", Proceedings of the First International Meeting on Wind Turbine Noise: Perspectives for Control, Berlin, October 2005.